Advances in Adaptive Data Analysis
Vol. 2, No. 4 (2010) 509–520

DOI: 10.1142/S1793536910000598

World Scientific
www.worldscientific.com

CONSTRUCTING CROSSOVER-FRACTALS USING INTRINSIC MODE FUNCTIONS

SY-SANG LIAW and FENG-YUAN CHIU

Department of Physics,
National Chung-Hsing University,
250 Guo-Kuang Road, 402 Taichung, Taiwan

Real nonstationary time sequences are in general not monofractals. That is, they cannot be characterized by a single value of fractal dimension. It has been shown that many real-time sequences are crossover-fractals: sequences with two fractal dimensions — one for the short and the other for long ranges. Here, we use the empirical mode decomposition (EMD) to decompose monofractals into several intrinsic mode functions (IMFs) and then use partial sums of the IMFs decomposed from two monofractals to construct crossover-fractals. The scale-dependent fractal dimensions of these crossover-fractals are checked by the inverse random midpoint displacement method (IRMD).

Keywords: Time sequence; fractal dimension; scaling exponent; crossover-fractal; trend.

PACS Number(s): 05.45.Tp, 05.40.-a, 05.45.Df

1. Introduction

Fractal dimensions or scaling exponents are considered to carry important information that the Fourier analysis fails to extract from a nonstationary time sequence. Among many kinds of methods, the detrended fluctuation analysis (DFA) [Peng *et al.*, 1994] is a popular method in calculating the Hurst exponents of time sequences in diverse fields of interest. From the value of Hurst exponents, we know that the time sequence is either nonautocorrelated or it correlates persistently or anti-persistently. It is generally believed that the Hurst exponent can also be related to the fractal dimension of the sequence in some definite way. With a single-scaling exponent in mind, though, researchers have found that in many cases [Penzel *et al.*, 2003; Havlin *et al.*, 1999; Scafetta *et al.*, 2006; Kavasseri and Nagarajan, 2004; Kantelhardt *et al.*, 2006; Liu *et al.*, 1997] time sequences have a crossover phenomenon. That is, they found that the Hurst exponent has two distinct values in the short and long ranges of time sequences. The crossover phenomenon has not gained much attention except for discussing the embedding of the fluctuations in a trend [Kantelhardt *et al.*, 2001; Hu *et al.*, 2001; Bashan *et al.*, 2008]. Recently, Scafetta and West (2009) had constructed crossover-fractals from noise via allometric filters and pointed out that the crossover-fractals, or even scale-dependent fractals, appear to

be more natural than do monofractals. In light of this, one is curious about how a crossover-fractal is formed, geometrically or dynamically. In this paper, we focus on the geometric construction of crossover-fractals.

It may be too naïve to think adding two monofractals will yield a crossover-fractal. Indeed, it does not work, but with a reason. Recently, we have developed a method named the inverse random midpoint displacement (IRMD), for determining fractal dimensions of time sequences [Liaw and Chiu, 2009]. The method and its modified version mIRMD [Liaw *et al.*, 2010] calculate the midpoint displacements that are linear combinations of data values (see Eq. (2)). Based on this simple linear formulation, we can understand why a superposition of two monofractals does not automatically become a crossover-fractal. Furthermore, thanks to the method of the empirical mode decomposition (EMD) [Huang *et al.*, 1998], we are able to extract necessary information from monofractals in order to construct crossover-fractals such that they have the fractal dimension of one monofractal in the short range and of the other in the long range.

The paper is organized as follows. We briefly summarized the method of mIRMD by demonstrating how it works on the Weierstrass function and the fractal Brownian motions (fBms) in Sec. 2. In Sec. 3, we stated the difficulty of constructing crossover-fractals from monofractals based on the formalism of the mIRMD. We next used EMD to decompose monofractals into components and found the fractal properties of each component using mIRMD. We then used these components to construct crossover-fractals. The problem of monofractals with a trend is considered in Sec. 4. Section 5 is the conclusion.

2. Calculation of the Fractal Dimensions

We will use two kinds of monofractals, the Weierstrass functions and fBms, for constructing crossover-fractals. The Weierstrass functions are given by the equation:

$$W(x) = \sum_{i=0}^{n} 2^{-i(2-D)} \cos(2^i x), \tag{1}$$

where D is the fractal dimension of the function and n is supposed to be infinity. A typical Weierstrass function $f(x) = W(x)$ of $D = 1.4$ calculated at $x = i/N$, $i = 0, 1, 2, \ldots, N$, $N = 2^{10}$ is plotted in Fig. 1. We calculated the average midpoint displacement $\langle G(s)\rangle$ at all scales s for this function [Liaw *et al.*, 2010]:

$$\langle G(s)\rangle = \frac{1}{N+1-s} \sum_{x=s/2}^{N-s/2} \left| f(x) - \frac{f(x-s/2) + f(x+s/2)}{2} \right|. \tag{2}$$

For monofractals, according to the mIRMD method [Liaw *et al.*, 2010], $\langle G(s)\rangle$ is proportional to s^{2-D} so that the fractal dimension[a] is given by 2 subtracted from

[a]For a monofractal of dimension D larger than 1, the average midpoint displacement $\langle G(s)\rangle$ is proportional to s^{2-D}. However, for a sequence of dimension $D = 1$, $\langle G(s)\rangle$ is proportional to s^H with $1 \le H \le 2$. We have shown [Liaw and Chiu, 2009; Liaw *et al.*, 2010] that for functions having second derivatives everywhere, H is equal to 2.

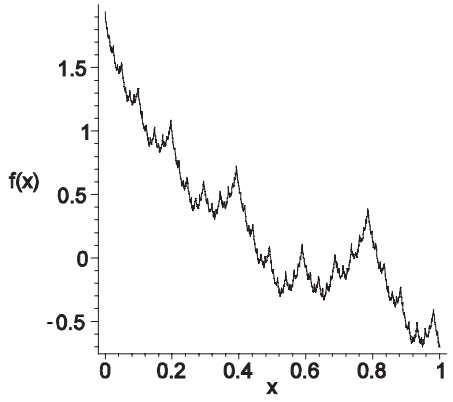

Fig. 1. A Weierstrass function of fractal dimension 1.4 represented by a time sequence of $N+1 = 2^{10}+1$ points at equal intervals $1/N$.

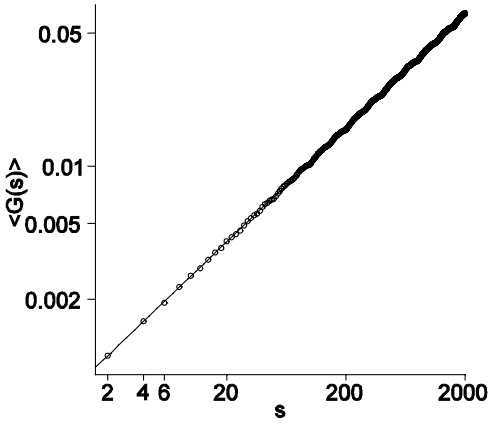

Fig. 2. Log-log plot of the average midpoint displacements $\langle G(s)\rangle$ versus scale s for the Weierstrass function of $D = 1.4$. The slope of the solid line is 0.600.

the slope of the linear fit for the plot of $\log(\langle G(s)\rangle)$ versus $\log(s)$. Figure 2 shows that the $\log(\langle G(s)\rangle)$ versus $\log(s)$ plot indeed yields very good results for the Weierstrass function.

The fBms of arbitrary fractal dimension can be easily generated using the method of random midpoint displacement (RMD) [Carpenter, 1980; Voss, 1985]. Given a value of the Hurst exponent H, $0 < H < 1$, the RMD begins with two arbitrary values at ends of an interval $[0, R]$: $f(0)$ and $f(R)$. We assign the value of $f(R/2)$ at the midpoint of the interval $[0, R]$ as the average of $f(0)$ and $f(R)$, plus a random value taken from a Gaussian distribution of standard deviation σ_0. Next, for the two non-overlapped intervals $[0, R/2]$ and $[R/2, R]$, we assign the value at the midpoint of each interval by the average of its end values plus a Gaussian random value of standard deviation $\sigma_1 = 2^{-H}\sigma_0$. Repeating the process M times by assigning values to the midpoints of 2^k non-overlapped intervals as the average of

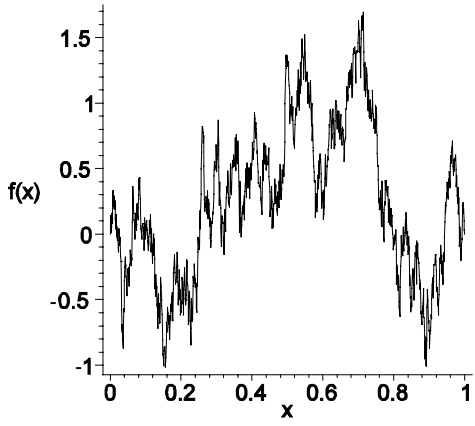

Fig. 3. A typical fBm of fractal dimension $D = 1.6$ generated by the RMD method.

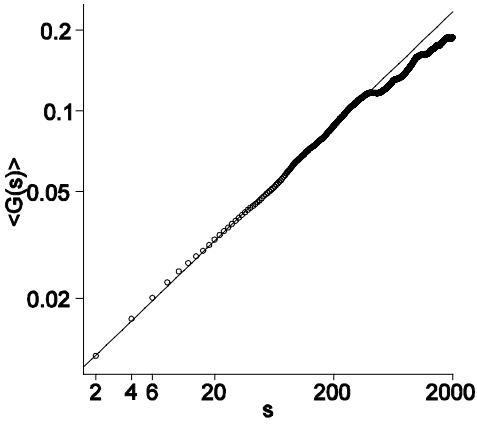

Fig. 4. Log-log plot of the average midpoint displacements $\langle G(s)\rangle$ versus scale s for the fBm of $H = 0.4$. The slope of the solid line is 0.428.

their end values plus a Gaussian random value of standard deviation $\sigma_k = 2^{-kH}\sigma_0$, we obtain a sequence of $2^M + 1$ points, which is an fBm with Hurst exponent H. A typical fBm, with the Hurst exponent $H = 0.4$, is plotted in Fig. 3. Its fractal dimension $D = 2 - H$ is calculated by mIRMD to yield $D = 1.572$ as shown in Fig. 4.

3. Constructing Crossover-Fractals

Let $\langle G_1(s)\rangle$ be the average midpoint displacement at scale s of a fractal $f_1(x)$ of dimension D_1 and $\langle G_2(s)\rangle$ be that of the fractal $f_2(x)$ of dimension D_2. What is the fractal dimension of the sum of $f_1(x)$ and $f_2(x)$: $h(x) = f_1(x) + f_2(x)$? The answer is: the function $h(x)$ can no longer be a monofractal — a fractal with

the same fractal dimension at all scales. If one uses mIRMD to plot $\log(\langle G(s)\rangle)$ versus $\log(s)$, the data points would not, in general, line up with a constant slope. Generalizing $\langle G(s)\rangle$ by interpolation to be a continuous function of s, we can then define the fractal dimension at scale s by the derivative of $\log(\langle G(s)\rangle)$ respective to $\log(s)$. A real fractal is, in general, not monofractal but a *scale-dependent fractal* that has different fractal dimensions at different scales [Carpena *et al.*, 2007]. A special kind of scale-dependent fractal has one fractal dimension for small scales and the other fractal dimension for scales larger than a certain value. We will call these fractals, *crossover-fractals*. The log-log plot of $\langle G(s)\rangle$ versus s for a crossover-fractal can be fitted by two line segments each having a distinct slope. Crossover-fractals have been observed in heart rate signals [Penzel *et al.*, 2003; Havlin *et al.*, 1999], in fluctuations of fatigue crack growth [Scafetta *et al.*, 2006], in wind speed data [Kavasseri and Nagarajan, 2004], in precipitation and river runoff records [Kantelhardt *et al.*, 2006], and in stock indexes at one minute intervals [Liu *et al.*, 1997; Liaw *et al.*, 2010]. Crossover-fractals can be constructed straightforwardly by the spectral method [Kantelhardt *et al.*, 2001]. Scafetta and West (2009) used allometric filters to generate crossover-fractals from noise. Below we will construct crossover-fractals using two given monofractals with the help of the EMD method [Huang *et al.*, 1998]. Before we do that, let us demonstrate a particular type of crossover-fractal that is handy. In calculating the Weierstrass function using Eq. (1), one would obtain a poor approximation if only a small number of terms, say $n = 12$, in the series are summed. Using mIRMD to calculate $\langle G(s)\rangle$ of this approximate Weierstrass function, we immediately see, from Fig. 5, that for a scale larger than a certain value $s > s_c$, the slope of $\log(\langle G(s)\rangle)$ respective to $\log(s)$ gives the correct fractal dimension of the Weierstrass function, but for $s < s_c$, the slope is close to 2, meaning that the approximate function behaves like a double differentiable

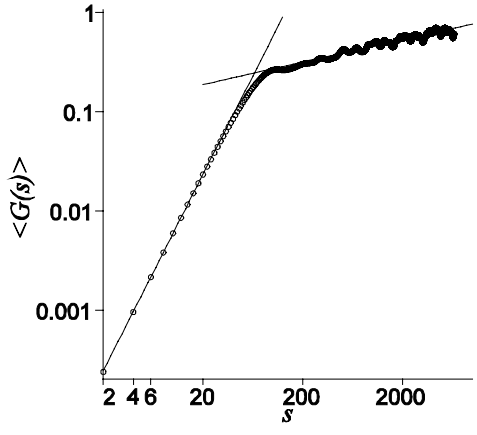

Fig. 5. Approximating the Weierstrass function ($D = 1.8$) by a finite series ($n = 12$ terms) yields a crossover-fractal which has a dimension of 1 at short ranges. The slopes of the two lines shown in the figure are 1.98 and 0.22, respectively.

function at small scales [Liaw and Chiu, 2009; Liaw *et al.*, 2010]. The value of the turning point s_c decreases as n increases. Weierstrass functions approximated by finite series are actually crossover-fractals.

Superposition of two monofractals will not automatically yield a crossover-fractal. This can be understood based on mIRMD. The fractal spectrum $D(s)$ of $h(x) = f_1(x) + f_2(x)$ is calculated through computation of $\langle G(s)\rangle$ according to Eq. (2):

$$\begin{aligned}\langle G(s)\rangle &= \frac{1}{N+1-s}\sum_{x=s/2}^{N-s/2}\left|h(x) - \frac{h(x-\frac{s}{2})+h(x+\frac{s}{2})}{2}\right| \\ &= \frac{1}{N+1-s}\sum_{x=s/2}^{N-s/2}\left|\left(f_1(x) - \frac{f_1(x-\frac{s}{2})+f_1(x+\frac{s}{2})}{2}\right)\right. \\ &\quad \left. + \left(f_2(x) - \frac{f_2(x-\frac{s}{2})+f_2(x+\frac{s}{2})}{2}\right)\right|. \qquad (3)\end{aligned}$$

Because we are taking absolute values in the sum, no simple relation can be found among $\langle G(s)\rangle$ and $\langle G_1(s)\rangle$ and $\langle G_2(s)\rangle$. Therefore, $D(s)$ cannot be a simple relation to D_1 and D_2. However, since the calculation of $\langle G(s)\rangle$ is linear in $f_1(x)$ and $f_2(x)$ and the contributions from the midpoint displacements of $f_1(x)$ and $f_2(x)$ are completely separated before taking an absolute value, $\langle G(s)\rangle$ would be determined by $f_1(x)$ alone if the displacements of $f_1(x)$ are much larger than that of $f_2(x)$ at scale s and vice versa. Note that the midpoint displacements of a monofractal $f(x)$ can be increased by any factor A, by simply multiplying $f(x)$ by A, without changing the fractal dimension of the function. Thus, by multiplying $f_1(x)$ with an appropriate constant A $(= \langle G(s_c)\rangle_{f_2}/\langle G(s_c)\rangle_{f_1})$, we are able to make the average midpoint displacements of $Af_1(x)$ equal to that of $f_2(x)$ at $s = s_c$ (Fig. 6). Assume $D_1 > D_2$, then the midpoint displacements of $Af_1(x) + f_2(x)$ approach that of $f_1(x)$ for $s \to 0$ and $f_2(x)$ for $s \to \infty$ as expected (Fig. 6). At any finite scale s, the fractal dimension of the superposed function is, in general, scale-dependent. To make a crossover-fractal with a fractal dimension D_1 for all scales $s < s_c$ and D_2 for all $s > s_c$ (or vice versa), we need the help of EMD.

The EMD is a general method for decomposing nonstationary data into bases derived from the data itself. Together with the Hilbert spectral analysis, they have been used extensively in geophysical research [Huang *et al.*, 1998]. An arbitrary nonstationary time sequence of N points can be decomposed by the EMD method into the sum of a set of finite number of intrinsic mode functions (IMFs), each of which is itself a time sequence of N points. Although each IMF does not have well-defined frequency, it carries a certain range of frequencies of the fluctuations of the original time sequence and can be ordered by their dominant frequencies. The appealing feature of EMD is that, starting with first IMF that represents the general trend, one can reveal the trend of the sequence with more details by adding more

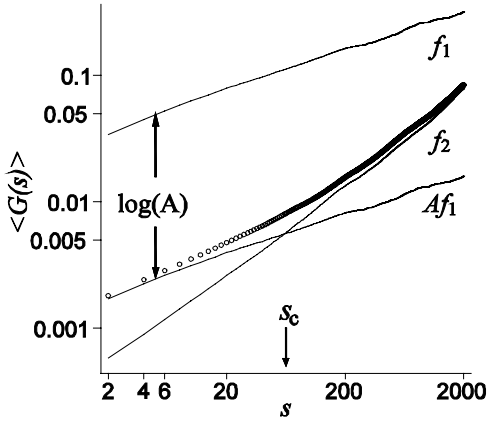

Fig. 6. Average midpoint displacements of a function can be changed linearly by multiplying the function with a constant. The fractal dimensions (circles) of the superposition of two arbitrary monofractals $(Af_1(x)+f_2(x))$ approach that of $f_1(x)$ and $f_2(x)$ at very short and very long scales, respectively.

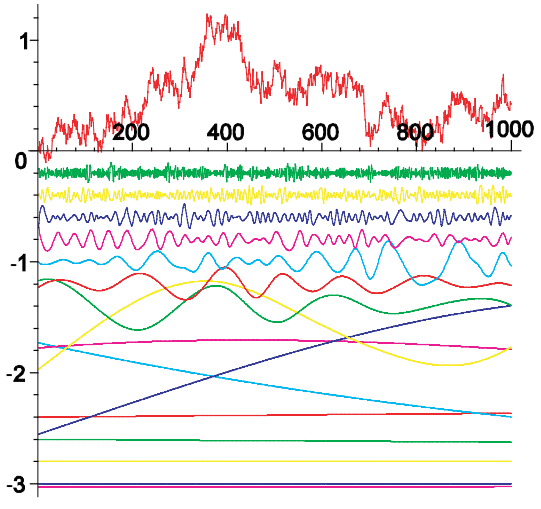

Fig. 7. An fBm of $D = 1.7$ (top) and its 16 IMFs arranged from the highest to lowest frequency by shifting each 0.2 further downward in the vertical scale for clarity.

IMFs one by one in order. Here we found, by calculating their fractal dimensions using mIRMD, that the IMFs of monofractal sequences have the unique property we need for constructing crossover-fractals. In Fig. 7, we show an fBm $f(x)$ of $D = 1.7$ and its 16 IMFs arranged from the lowest to highest frequency.[b] We made

[b]We used the MATLAB codes eemd.m downloaded from the RCADA Web site http://rcada.ncu.edu.tw/research1.htm to generate IMFs.

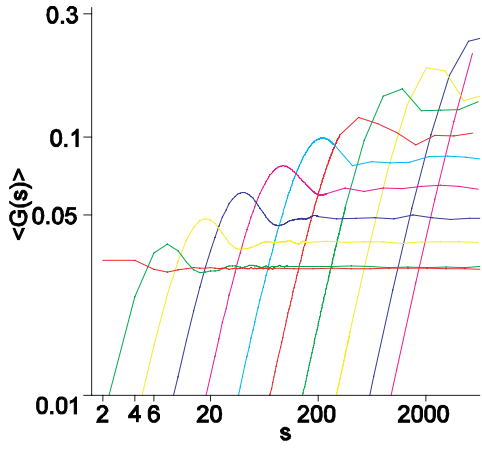

Fig. 8. Average midpoint displacements as a function of scale for 10 high frequency IMFs. Each curve has a slope = 2 (double differentiable) in the small scales and slope = 0 (white noise) in the large scales.

the $\log(\langle G(s)\rangle)$ versus $\log(s)$ plots for 10 high frequency IMFs in Fig. 8 to show that each IMF carries fractal information within a certain small range of scales, below which it behaves like a double differentiable function (slope = 2, $D = 1$) and above like white noise (slope = 0, $D = 2$). These resultant curves of mIRMD for all IMFs except the first one collapse approximately into a single curve by a simple scale transformation. The result is consistent with the previous finding that the Fourier spectra of all IMFs except the first one can be rescaled to overlap one another [Wu and Huang, 2004; Flandrin *et al.*, 2004]. The unique property of the IMFS allows us to build fractals with designated scale-dependent dimensions. For example, the accumulate IMFs up to a certain frequency of fluctuation, denoted by, $f^{\text{up}}(x)$ are a crossover-fractal with $D = 1$ for small scales and $D = 1.7$ for large scales. On the other hand, the accumulate IMFs down to a certain frequency of fluctuation, denoted by $f^{\text{down}}(x)$, are also a crossover-fractal, but with $D = 1.7$ for small scales and $D = 2$ for large scales (Fig. 9).

Now, for two given functions $f_1(x)$ and $f_2(x)$ with dimensions D_1 and D_2 respectively, we use EMD to decompose them and then make $f_1^{\text{down}}(x)$ and $f_2^{\text{up}}(x)$, so that the average midpoint displacements of both of these two crossover-fractals have turning points around the same scale s_c. Below s_c, $\log(\langle G(s)\rangle)$ of $f_2^{\text{up}}(x)$ decreases much faster than that of $f_1^{\text{down}}(x)$ as s decreases. Above s_c, $\log(\langle G(s)\rangle)$ of $f_1^{\text{down}}(x)$ is almost constant while that of $f_2^{\text{up}}(x)$ keeps increasing with s. Define the function $h(x)$, $h(x) = Af_1^{\text{down}}(x) + f_2^{\text{up}}(x)$, where A is the appropriate factor that makes the displacements of $Af_1^{\text{down}}(x)$ and $f_2^{\text{up}}(x)$ equal at the chosen scale s_c. The function $h(x)$ will then be a crossover-fractal with $D = D_1$ for $s < s_c$ and $D = D_2$ for $s > s_c$, since for $s < s_c$ the average midpoint displacements of $Af_1^{\text{down}}(x)$ are much larger than that of $f_2^{\text{up}}(x)$, and for $s > s_c$ the displacements of $Af_1^{\text{down}}(x)$ are much smaller than that of $f_2^{\text{up}}(x)$. Similarly, we can construct a crossover-fractal

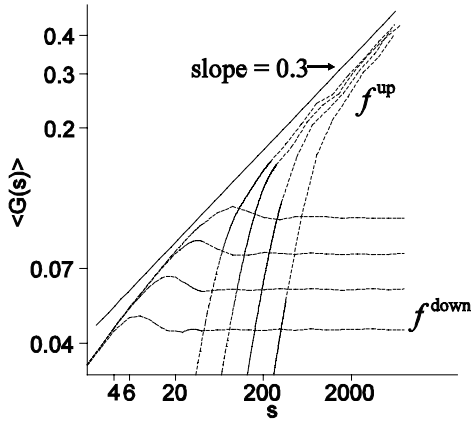

Fig. 9. Average midpoint displacements as a function of scale for accumulate IMFs: $f^{\mathrm{up}}(x)$ of 8, 9, 10, and 11 IMFs, respectively (dashed curves) and $f^{\mathrm{down}}(x)$ of 2, 3, 4, and 4 IMFs, respectively (dotted curves).

with $D = D_2$ for $s < s_c$ and $D = D_1$ for $s > s_c$ by simply adding $Af_1^{\mathrm{up}}(x)$ and $f_2^{\mathrm{down}}(x)$.

As a demonstration, we generate an fBm of $D_1 = 1.3$ and another of $D_2 = 1.7$. Let the sum of the IMFs of the first four highest frequencies of the former fBm be $f_1^{\mathrm{down}}(x)$, and the sum of the last 12 IMFs be $f_1^{\mathrm{up}}(x)$. Similarly, we obtain $f_2^{\mathrm{down}}(x)$ and $f_2^{\mathrm{up}}(x)$ in the same manner (the constant A has been chosen appropriately and absorbed in $f_1(x)$). We check their crossover-fractal properties using

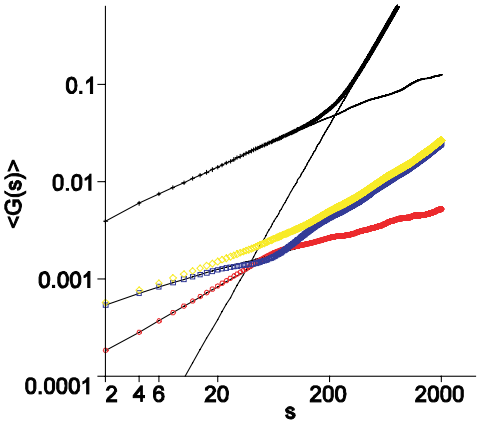

Fig. 10. Calculation of the fractal dimensions of the crossover-fractals using mIRMD. $f_1(x)$ and $f_2(x)$ are monofractals with dimensions 1.3 and 1.7, respectively. Results for the sequences $f_1(x) + f_2(x)$, $f_1^{\mathrm{up}}(x) + f_2^{\mathrm{down}}(x)$, and $f_1^{\mathrm{down}}(x) + f_2^{\mathrm{up}}(x)$ are indicated by the symbols diamond, square, and circle, respectively. The superposition of a monofractal fBm of dimension 1.5 (line with slope 0.5) and a double differentiable trend $t(x) = Ax^2$, $A = 2^{-18}$ (line with slope 2.0) is approximately a crossover-fractal (cross).

mIRMD (Fig. 10). We see they are indeed well-defined crossover-fractals as designed except within a small range in the neighborhood of s_c.

4. Monofractals with a Trend

Consider a monofractal embedded in a trend: $h(x) = f(x) + At(x)$, where $f(x)$ is a monofractal of dimension D_1 and $t(x)$ a double differentiable trend. Because $t(x)$ is of dimension 1 and has second derivatives everywhere, its log-log plot of average displacement versus scale has slope 2, which is much larger than the slope $2-D_1 < 1$ for $f(x)$. Therefore, the average midpoint displacement of $h(x)$ is dominant by the contributions from $f(x)$ and $At(x)$ respectively, for the scales smaller and larger than a certain s_c (Fig. 10), which value is adjustable by varying the amplitude A. Thus, the superposition of a monofractal and a trend is a very good approximation of a crossover-fractal that exhibits a fractal property of the monofractal in short ranges and shows as a smooth trend in long ranges.

Note that the short-range fractal dimension of the time series $h(x)$ is always D_1 with or without the trend, and a double differentiable trend is immediately revealed by identifying a line of slope = 2 in the long-range region in the double log plot of average displacement versus scale. Methods such as DFA and its other extensions are designed to eliminate the contributions of the trend in order to reveal the intrinsic fractal dimensions at long scales. However, if a trend can never be removed from a real-time series itself, there is no point to find its intrinsic fractal dimensions in the long ranges since the real long-range correlation is mainly determined by the trend. The merit of the detrending procedures that are used in DFA and others is thus not to reveal long-range correlation of a time series [Kantelhardt *et al.*, 2001; Hu *et al.*, 2001] but to see whether or not there is a simple trend. A complex trend other than simple polynomials cannot be removed, in general, without changing the embedded fractals.

For real nonstationary data, in addition to indentifying its trend, it is also very important to extract unwanted noise [Kantz and Schreiber, 1997; Bottcher *et al.*, 2006]. From our construction of the crossover-fractals described above, we see that a white noise embedded in the data can be easily identified from the log-log plot of $\langle G(s)\rangle$ versus s since it has dominant contribution in the small scales.

5. Conclusion

Fractal dimensions of a nonstationary time series are in general scale-dependent. We used a modified method of IRMD to calculate the average midpoint displacements $\langle G(s)\rangle$ of intervals of length s and obtained the fractal spectrum $D(s)$ from the slope of the double log plot of $\langle G(s)\rangle$ versus s. The simplest scale-dependent fractals are the crossover-fractals that have one fractal dimension for small scales and the other fractal dimension for scales larger than a certain value. With the help of the method of the EMD, we were able to construct crossover-fractals from two monofractals.

We also showed that a monofractal embedded in a double differentiable trend can be well approximated by a crossover-fractal.

Acknowledgments

This work is supported by grants from the National Science Council under the grant number NSC97-2112-M005-001, and the National Center for Theoretical Sciences of Taiwan.

References

Bashan, A., Bartsch, R., Kantelhardt, J. W. and Havlin, S. (2008). Comparison of detrending methods for fluctuation analysis. *Physica*, **A387**: 5080–5090.

Bottcher, F., Peinke, J., Kleinhans, D., Friedrich, R., Lind, P. G. and Haase, M. (2006). Reconstruction of complex dynamical systems affected by strong measurement noise. *Phys. Rev. Lett.*, **97**: 090603.

Carpena, P., Bernaola-Galvan, P., Coronado, A. V., Hackenberg, M. and Oliver, J. L. (2007). Identifying characteristic scales in the human genome. *Phys. Rev.*, **E75**: 032903.

Carpenter, L. (1980). Computer rendering of fractal curves and surfaces. *Comput. Graph.*, 109ff.

Flandrin, P., Rolling, G. and Gonalvs, P. (2004). Empirical mode decomposition as a filter bank. *IEEE Signal Process. Lett.*, **11**: 112–114.

Havlin, S., Amaral, L. A. N., Ashkenazy, Y., Goldberger, A. L., Ivanov, P. Ch., Peng, C.-K., and Stanley, H. E. (1999). Application of statistical physics to heartbeat diagnosis. *Physica*, **A274**: 99–110.

Hu, K., Ivanov, P. Ch., Chen, Z., Carpena, P. and Stanley, H. E. (2001). Effects of trends on detrended fluctuation analysis. *Phys. Rev.*, **E64**: 011114.

Huang, N. E., Shen, Z., Long, S. R., Wu, M. C., Shih, H. H., Zheng, Q., Yen, N. Y., Tung, C. C. and Liu, H. H. (1998), The empirical mode decomposition and the Hilbert spectrum for nonlinear and non-stationary time series analysis. *Proc. R. Soc. London, Ser. A*, **454**: 903–993.

Kantelhardt, J. W., Koscielby-Bunde, E., Rego, H. H. A., Havlin, S. and Bunde, A. (2001). Detecting long-range correlations with detrended fluctuation analysis. *Physica*, **A295**: 441–454.

Kantelhardt, J. W., Koscielny-Bunde, E., Rybski, D., Braum, P., Bunde, A. and Havlin, S. (2006). Long-term persistence and multifractality of precipitation and river runoff records. *J. Geophys. Res.*, **111**: D01106.

Kantz, H. and Schreiber, T. (1997). *Nonlinear Time Series Analysis* (Cambridge University Press, Cambridge, England).

Kavasseri, R. G. and Nagarajan, R. (2004). Evidence of crossover phenomena in wind-speed data, *IEEE Trans. Circuits Syst., Part I: Fundamental Theory and Applications*, **51**: 2255–2262.

Liaw, S.-S. and Chiu, F.-Y. (2009). Fractal dimensions of time sequences. *Physica*, **A388**: 3100–3106.

Liaw, S.-S., Chiu, F.-Y., Wang, C.-Y. and Shiau, Y.-H. (2010). Fractal analysis of stock index and electrocardiograph. *Chin. J. Phys.*, **48**(6), in press.

Liu, Y., Cizeau, P., Meyer, M., Peng, C.-K. and Stanley, H. E. (1997). Correlations in economic time series. *Physica*, **A245**: 437–440.

Peng, C.-K., Buldyrev, S. V., Havlin, S., Simons, M., Stanley, H. E, and Goldberger, A. L. (1994). Mosaic organization of DNA nucleotides, *Phys. Rev.*, **E49**: 1685–1689.

Penzel, T., Kantelhardt, J. W., Becker, H. F., Peter, J. H. and Bunde, A. (2003). Detrended fluctuation analysis and spectral analysis of heart rate variability for sleep stage and apnea identification, *Comput. Cardiol.*, **30**: 307–310.

Scafetta, N., Ray, A. and West, B. J. (2006), Correlation regimes in fluctuations of fatigue crack growth, *Physica*, **A359**: 1–23.

Scafetta, N. and West, B. J. (2009). Emergence of bi-fractal time series from noise via allometric filters, *Euro. Phys. Lett.*, **79**: 30003.

Voss, R. F. (1985), in: *Fundamental Algorithms in Computer Graphics*, ed. R. A. Earnshaw (Springer, Berlin), pp. 805–835.

Wu, Z. and Huang, N. E. (2004). A study of the characteristics of white noise using the empirical mode decomposition method, *Proc. R. Soc. London*, **460A**: 1597–1611.